Springer

KSME

Journal of Mechanical Science and Technology 31 (8) (2017) 3793~3801
www.springerlink.com/content/1738-494x(Print)/1976-3824(Online)
DOI 10.1007/s12206-017-0723-y

Characteristics of Al/steel magnetic pulse tubular joint according to discharging time †

Ji-Yeon Shim[1], Bong-Yong Kang[1,*] and Ill-Soo Kim[2,*]

[1]*Carbon & Light Materials Application R&D Group, KITECH, Korea*
[2]*Department of Mechanical Engineering, Mokpo National University, Korea*

(Manuscript Received October 12, 2016; Revised January 15, 2017; Accepted March 3, 2017)

Abstract

The MPW (Magnetic pulse welding) process is governed by the electromagnetic force that results from electromagnetic interaction produced by a coil. To produce high electromagnetic force, the MPW process needs to charge high electrical energy through capacitors. The total capacitance and system inductance has an effect on the discharge time, and discharge time also has an effect on the joint. Therefore, the objective of this research is to analyze the effect of the discharge time on the joint and to quantify it using the FE-model. To achieve this, MPW has been performed using Al1070tube and S45Crod. After the experiment, the interfaces of the joint with variations of discharge time were observed utilizing a scanning electron microscope. In addition, a two dimensional electromagnetic-mechanical coupled FE-model has been developed for quantification. Experimental results demonstrated the impact of welded interfaces that have various lengths and amplitudes. It was confirmed from the numerical works that the creation of a wavy form is derived from the change of electromagnetic force according to the variation of discharge time. As the discharge time decreased, the lengths and amplitudes of the wave form decreased through the reduction of the generated electromagnetic force.

Keywords: Aluminum welding; Electromagnetic force; Dissimilar materials welding; Joint interface

1. Introduction

In the field of automotive engineering, lightweight constructions of components are being developed for fuel-efficiency savings and environment-friendly manufacturing processes. To achieve these very different goals, lightweight materials, such as Aluminum (Al) and Magnesium (Mg), have been applied for components. In particular, the development of aluminum space frames for automotive body structures has been carried out in recent years [1, 2]. However, when only lightweight materials are used in automotive components, the materials cannot satisfy the required strength; hence, it is imperative to weld between lightweight materials and currently used materials, such as steel. Accordingly, it has become necessary to study the welding of dissimilar metals that have different material properties. The fusion welding process by heat generally causes not only defects, such as solidification, cracking, porosity, and oxidation, but also transformation and corrosion. Therefore, magnetic pulse welding as a kind of solid-state welding process has recently been developed [1-5].

MPW was developed for military applications, such as the joining of projectiles to artillery shell castings in the former Soviet Union 40 years ago [3, 4]. The theoretically impact velocity of the MPW process was reported to be 15000 m/s, but, generally, the impact velocity is limited to less than 1000 m/s by the developed power source and working coil [6]. The process closely analogizes with explosive welding. However, rather than explosives, it uses electromagnetic force to impact between workpieces so that it can improve the productivity and the safety of the worker. With proper design, the generated electromagnetic force is fairly efficiently used for accelerating the outer workpiece rather than heating or melting the materials [7]. As no heat is applied to the workpiece, defects do not occur and a high-quality joint can be obtained. Because of its advantages, for several years, researchers have been experimentally and numerically studying the MPW process for tubular welding with a variety of similar and dissimilar material combinations. Recently, study on the effect of the process parameters using the MPW process has been carried out by various researchers. Generally, MPW process parameters were reported the charged voltage and the gap between workpieces. Kapil et al. [8] and Raoelison et al. [9] showed the weldability windows, which mean the critical range of process parameters for achieving the successful joint. Additionally, Bellmann et al. [10] represented the effect of

*Corresponding authors. Tel.: +82 61 450 2416, +82 63 210 3710, Fax.: +82 61 454 3455, +82 63 210 3700
E-mail address: ilsookim@mokpo.ac.kr, kanbo@kitech.re.kr
† Recommended by Associate Editor Hak-Sung Kim

surface coating on the tubular joint. However, when this process is examined to apply the prototype as industry components, deformation of the inner workpiece occurs through high-velocity impact, which causes a poor joint. Therefore, Cui et al. [11] carried out studies on the influence of the thickness of Al/Steel tube on the joint quality and Lueg-Althoff et al. [12] studied this with an Al/Cu tube. The critical thickness of the tube depended on the discharging voltage in these researches. Ben-Artzy et al. [13, 14] reported the characteristics of interfacial wave formation according to the thickness of the tube.

Because the MPW process only uses electromagnetic force that is generated by the electromagnetic interaction between the coil and outer workpiece, FEM (Finite elements method) is often employed for analyzing the process. Kore et al. [15] studied the effect of the process parameters on the joint using the FE-model, and Geng et al. [16] investigated the critical thickness of the inner tube for MPW using FEM. However, this research has attempted to achieve the joint with the minimum discharge time during the process simply, and analysis of the effect of discharge time was not carried out. However, the electromagnetic interaction during the process is governed by the discharge time as equations of the MPW system, which consists of capacitance, inductance, and resistance. Moreover, plastic deformation of workpieces results from this electromagnetic interaction. Because research on the effect of discharge time on peak current in the MPW process has not been documented and in that sense, the primary objective of this paper is to analyze the effect of discharge time on the joint and to quantify the electromagnetic interaction and deformation behavior. The MPW processes in this study employed an Al tube and a carbon steel rod, and the results of the experimental and numerical works were obtained through the analysis of the observed interface of the joint and developed FE-model, respectively. It is anticipated that this research will contribute to selection of the proper discharge time and to improving the understanding of electromagnetic interaction and deformation behavior according to the variation of discharge time.

2. Experimental works

2.1 Principle of the MPW

MPW is a high-speed solid-state welding process that is accomplished by an electromagnetic force causing a high-velocity impact on two workpieces, resulting in a true metallurgical bond [17]. Fig. 1 shows the schematic illustration of the MPW process. An electrical discharge circuit is applied to the present welding. The circuit consists of a power source as a capacitor bank, a high-current discharge switch, and a working coil. The workpieces are inserted into the coil, so they overlap each other. When a high-pulse current from the power source passes through the working coil, a high magnetic field is instantaneously generated around the coil. At that time, an eddy current is induced on the outer workpiece surface. The induced eddy current flows in the opposite direction of the working coil and then leads to a high electromagnetic force.

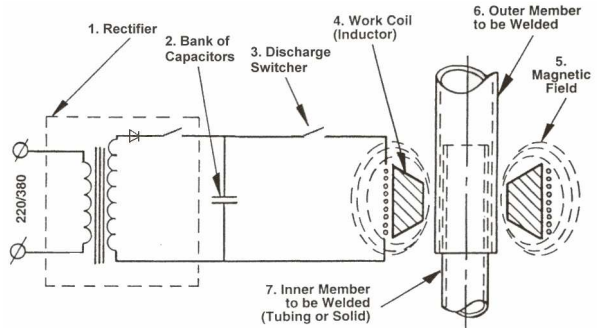

Fig. 1. Schematic illustration of the MPW process [18].

This electromagnetic force is applied on the outer workpiece, which leads to impact with the inner workpiece at nearly 1000 m/s [18].

The total charge energy of capacitor can be calculated using Eq. (1)

$$E = \frac{1}{2}CV^2 \tag{1}$$

where E is the total charge energy in joules, C the total capacitance in μF, and V is the charge voltage in volts. The current discharged through the coil can be described by the following differential Eq. (2):

$$\frac{d^2I(t)}{dt^2} + 2\xi\omega\frac{dI(t)}{dt} + \omega^2 I(t) = 0 \tag{2}$$

$$\xi = \frac{1}{2}R_a\sqrt{\frac{C}{L_a}} \tag{3}$$

$$\omega = \sqrt{\frac{1}{L_a C}} = 2\pi f \tag{4}$$

where I is the current in amperes, t is the time in seconds, ω is angular frequency, ξ is damping ratio R is the resistance in ohms, C is the capacitance in farads, and f is the frequency in hertz.

$$R_a = R_{coil} + R_{power\ supply} \tag{5}$$

$$L_a = L_{coil} + L_{power\ supply} \tag{6}$$

where L is the inductance in henries. The discharge current profile is given by this equation, and it oscillates between positive and negative values and decays with time [18, 19].

2.2 Experimental procedures

As shown in Fig. 2, MPW system manufactured by Welmate Co., Ltd. was employed for this study. This MPW system consisted of a magnetic pulse power source and a single turn coil. The power source was based on the capacitors, which consisted of 10 capacitors connected in parallel. The capacitors were discharged to the coil by 10 triggered switch

Table 1. Welding condition.

#	Capacitance (μF)	Charge voltage (kV)	Charge energy (kJ)
Case A	720	8.6	26.6
Case B	840	8	26.8
Case C	960	7.5	27

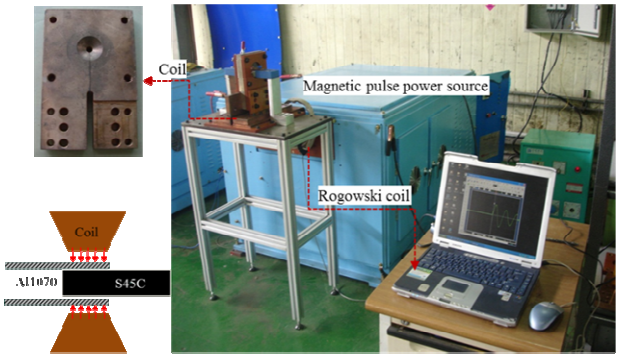

Fig. 2. Experimental set-up for MPW system.

units. The total capacitance was 1200 μF, and the charging voltage was up to 10 kV. The welding condition, which was decided by the variation of capacitance under the same charge energy, is shown in Table 1.

The workpieces for the experiment employed a 0.7 mm thick aluminum alloy tube (Al070) as the outer workpiece and an 8 mm-diameter structural carbon steel rod (S45C) as the inner workpiece. Hereafter, they are called the Al tube and the S45C rod, respectively. The material surface was cleaned with alcohol and dried. No special surface treatment was applied before welding. The prepared materials were inserted into the welding coil, and it was overlapped at a length of 10.5 mm. In particular, the gap of the Al tube, which was the outer workpiece with high electrical conductivity, and the coil always maintained 1.0 mm for high electromagnetic interaction. The Rogowski coil for measuring the currents during the discharge time was set at the connection part between the pulse power source and the coil. The Rogowski coil can measure the current linearly from a low current to a high current using mutual inductance. Moreover, it can measure the current in a wide frequency range. After welding, the helium leakage test was carried out for the evaluation of the joint, and then the interfaces were precisely examined using an optical metallographic microscope and SEM (Scanning electron microscope).

2.3 Results and discussion

Fig. 3 shows the obtained wave form by the Rogowski coil. Thus, the MPW process only uses a quarter of the cycle, which means up to the peak current on the measured wave from. This is because when the generated electromagnetic force through the coil is applied on the workpiece, plastic deformation starts, and it ends as the gap between the coil and workpiece is increased by low electromagnetic interaction

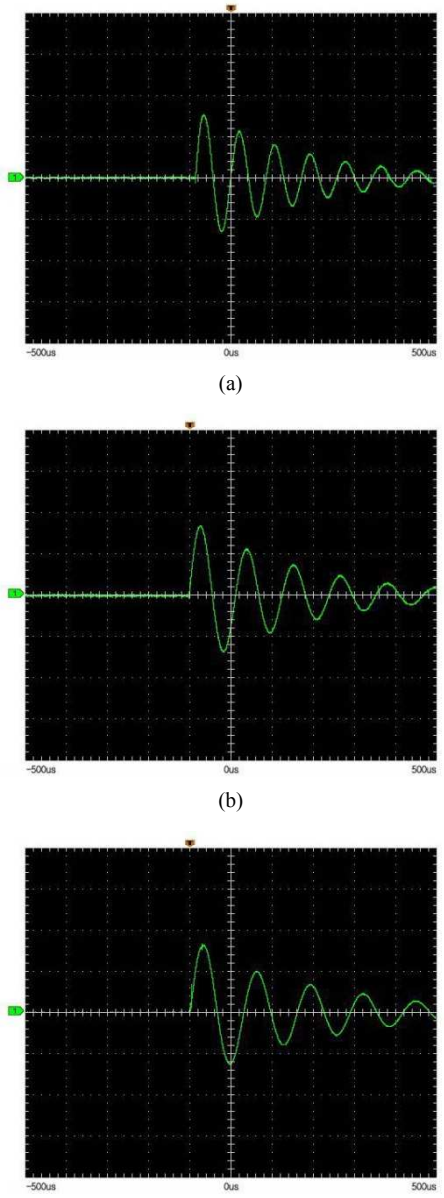

Fig. 3. Discharge waveform (X: 100 μs/div, Y: 5 v/div) with a calibration coefficient of 44.5 kA/v: (a) Case A; (b) case B; (c) case C.

between the coil and Al tube. The damped sinusoidal waveform was measured similarly under different capacitances, and the peak current was measured as approximately 400 kA. However, the discharge time to peak current was measured as 20 μs, 25 μs and 30 μs under the capacitances of 720 μF, 840 uF and 960 μF, respectively, as shown in Table 2.

The joints, which were successfully welded in all the cases, were tested for helium leakage. The leak rates of cases A and B were 5.6×10^{-11} mbar$\cdot$l$\cdot$s^{-1} and 5.6×10^{-11} mbar$\cdot$l$\cdot$s^{-1}, respectively. However, the leak rate of case C was measured as 5.6×10^{-11} mbar$\cdot$l$\cdot$s^{-1}, which was sharply decreased compared with other cases. For the analysis of the interface characteristics of the joints, the joints were cut along the longitudi-

Table 2. Discharge time according to variation of capacitance.

#	Capacitance (μF)	Charge voltage (kV)	Discharge time (μs)
Case A	720	8.6	20
Case B	840	8	25
Case C	960	7.5	30

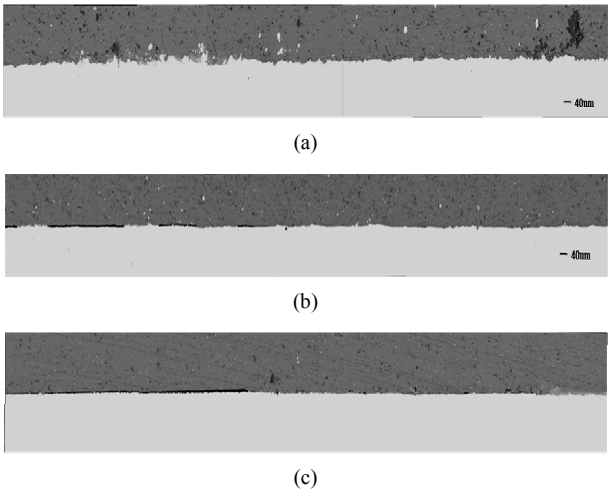

(a)

(b)

(c)

Fig. 4. Interface of joint with variation of discharge time: (a) Case A; (b) case B; (c) case C.

nal weld region and then were observed using an optical microscope, as in Fig. 4, which shows the interface of the joint in different MPW conditions. In all cases, the wavy forms were observed as shown in Fig. 5. Such interfacial morphology has been reported for a high-speed impact joint, such as in explosive welding.

These wavy forms mean the metallurgical joining of materials through high-velocity impact. In accordance with the Kelvin-Helmholtz instability model, the materials are influenced by hydrodynamics during joining. When the two fluids with different material properties with different velocities interact, instabilities occur at the interface as a result of the interferences. These instabilities involve mass flow, usually from the higher density material to the lower one. Whenever instability occurs, it has a direction and a certain velocity (energy), and it causes a movement of the material from one side of the interface to the other [14]. This confirms that the MPW process can achieve a high-quality joint and that there is no sign of a heat-affected zone. The lengths and amplitudes of the wavy forms were observed in the two weld zones on the interface. The length of the wave form was measured as 2 mm in case A, but the wave did not form continuously in case B and case C. The amplitudes of the wavy forms on the welding starting part were observed to be approximately 20 μm in case A. However, the amplitudes of case B were less than 10 μm, and wavy forms in case C were rarely observed. According to these results, by decreasing the discharge time, the wavy form length was longer and the amplitude was higher. To analyze the effect of the discharge time on the interface, numerical

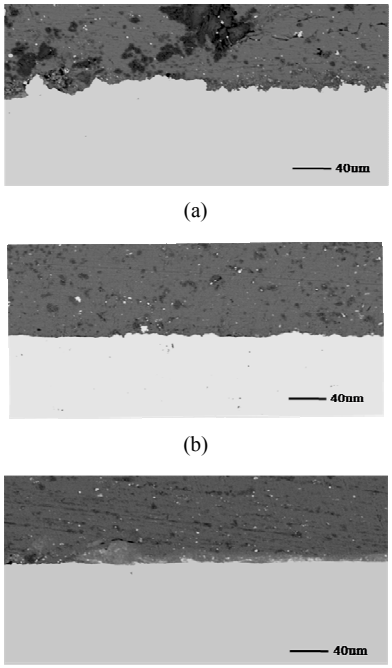

(a)

(b)

(c)

Fig. 5. Wavy form with variation of discharge time: (a) Case A; (b) case B; (c) case C.

works are performed in Sec. 3.

3. Numerical works

3.1 Analysis method and procedure

MPW is performed by the high-speed collision that occurs as the outer workpiece flies towards the inner workpiece using the electromagnetic force generated in the electromagnetic interaction between the coil and the workpiece. Since the electromagnetic force is calculated based on the discharge current, induced eddy current, and magnetic flux density generated in the workpiece and coil during the process, electromagnetic simulation is indispensable to numerically analyze the MPW process. In addition, it is possible to predict the shape of the joint by accurately identifying the electromagnetic force and how its distribution acts on the outer workpiece based on the result of numerically measuring the electromagnetic phenomena occurring within tens of microseconds (μs), which was difficult to measure in the experiment. To simulate the transient electromagnetic phenomena, a commercially available finite element software package, ANSYS EMAG, was used. Additionally, the impact behavior of the workpieces was modeled using the commercial software package LS-DYNA, an explicit dynamic finite element program [20-22] for solving the high speed impact problem effectively. Fig. 6 shows a schematic diagram of the numerical works. During the simulation, the electromagnetic forces, which were applied on the Al tube through electromagnetic interaction, were calculated from the electromagnetic model, and then the calculated electromagnetic forces were used as an input load to simulate the

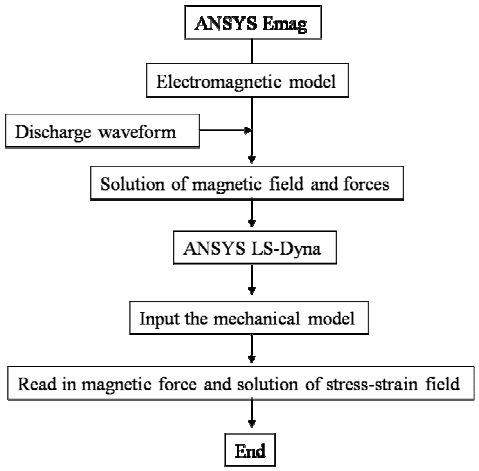

Fig. 6. Schematic diagram of numerical works.

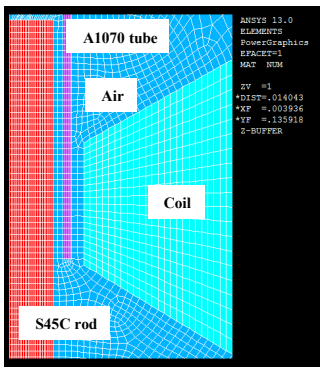

Fig. 7. 2D FE-model for this research.

high-velocity deformation of the Al tube from the mechanical mode.

Fig. 7 shows the 2D FE-model for this research. Because of the problem of symmetry, only a quarter of the workpieces and the coil were modeled. The workpiece and coil were modeled using the same experiment dimensions and material properties. The following electrical properties for the coil were inputted: A Poisson's ratio of 0.343, 1 μ permeability, and 1.7e-006 Ohm-cm resistivity. According to the measured values, a current of 400 kA was inputted into the coil as a sine wave function during the simulation. The boundary conditions can be established as follows [20]:

(a) $\underset{B}{\rightarrow}$ (Magnetic induction intensity) is perpendicular to x axis at $y = 0$ in the Cartesian coordinate system.

(b) $\underset{A}{\rightarrow}$ (Vector magnetic potential) is equal to zero at $x = 0$ in the Cartesian coordinate system.

(c) An infinite flag is set on the outer line of the far-field air region in the Cartesian coordinate system.

To enhance the accuracy of the calculation and to reduce the analysis time, plane13, which has four nodes with up to four degrees of freedom per node, was utilized with a mapped mesh with 160073 nodes and 78116 elements in total. Table 3 shows the material properties for this simulation.

Table 3. Material properties for numerical works.

Material	Resistivity $(\Omega \cdot m)$	Tensile strength (MPa)	Yield strength (MPa)
A1070 (Outer workpiece)	3.4e-8	70	45
S45C (Inner workpiece)	1.0e-7	686	490
C12200 (Coil)	2.17e-8	330	300

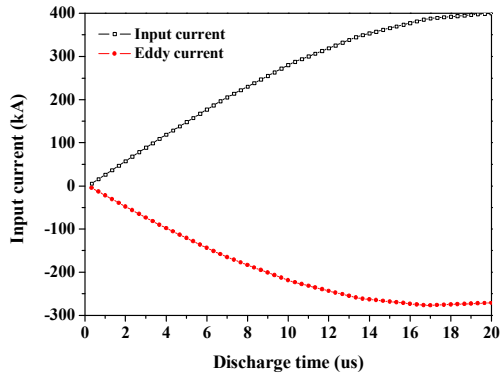

(a)

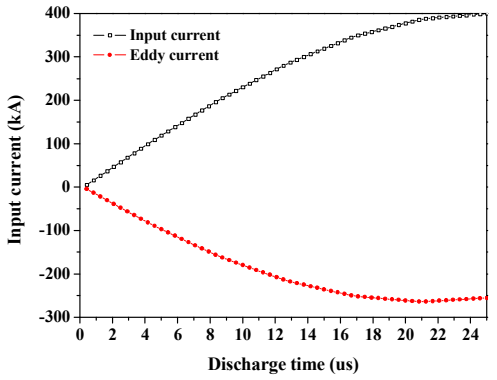

(b)

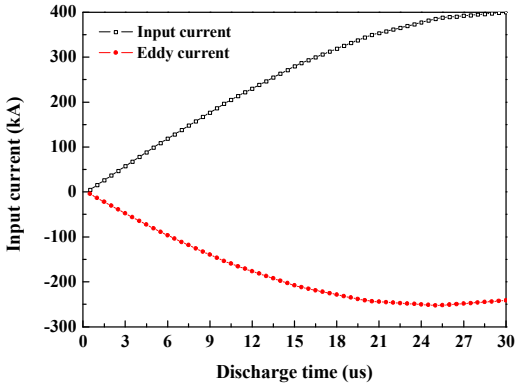

(c)

Fig. 8. Eddy currents with variation of discharge time: (a) Case A (Discharge time = 20 μs); (b) case B (Discharge time = 25 μs); (c) case C (Discharge time = 30 μs).

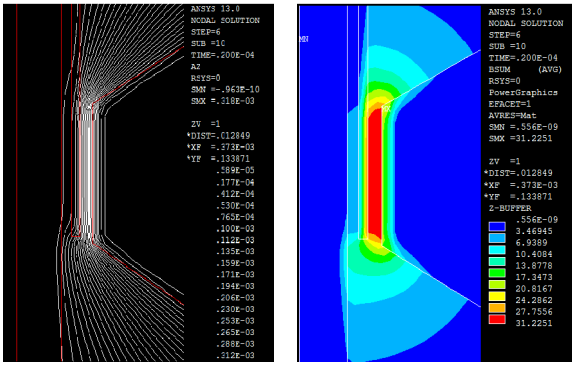

(a) (b)

Fig. 9. The electromagnetic interaction during the MPW process: (a) Distribution of flux line; (b) contour of magnetic flux density.

3.2 Results and discussion

The eddy current when the 400 kA peak current was inputted into the coil for the 20 μs discharge time generated 276.8 kA, and the discharge times at 25 μs and 30 μs were calculated to be 264 kA and 252.3 kA, respectively, as shown in Fig. 8. From these results, it was confirmed that the eddy currents generated about 70 % of the input currents and the reaction of these currents, which has each opposite direction, caused the high electromagnetic force. By decreasing the discharge time, the eddy currents were decreased, and the difference between case A and case C in the induced eddy current was 24.5 kA. Fig. 9(a) shows the distribution of the magnetic flux line between the coil and Al tube when the eddy currents were induced on the Al tube surface. The flux line is centralized adjacent to the gap between the coil and Al tube. In particular, the magnetic flux density was centralized on the exterior angle of the coil surface due to the skin effect. Fig. 9(b) illustrates the magnetic flux density. For the analysis of the distribution of the magnetic flux density as time passes, each discharge time was divided by three time steps. When 400 kA was inputted into the coil, the maximum magnetic flux densities for 20 μs, 25 μs and 30 μs were calculated to be 28.4 T, 27.7 T and 27.1 T, respectively, as shown in Fig. 10.

These magnetic flux densities, which are shown in Fig. 10, were caused by the magnetic force of the high-speed impact between the workpieces. Fig. 11 shows a vector plot of the magnetic force at the 20 μs discharge time compressing from the Al tube surface to the S45C rod.

Fig. 12 shows the distribution of magnetic force with the variation of discharge time. The contours of magnetic force were comparatively similar, but the values of magnetic force at 20 μs increased sharply. The maximum force was calculated to be 901 N at 20 μs. In contrast, the maximum values were 791 N and 714 N at 25 μs and 30 μs, respectively. The difference between case A and case C in force was about 187 N.

The yield stress of the workpieces was exceeded by the acting force, and the strongly dynamic deformation started. In

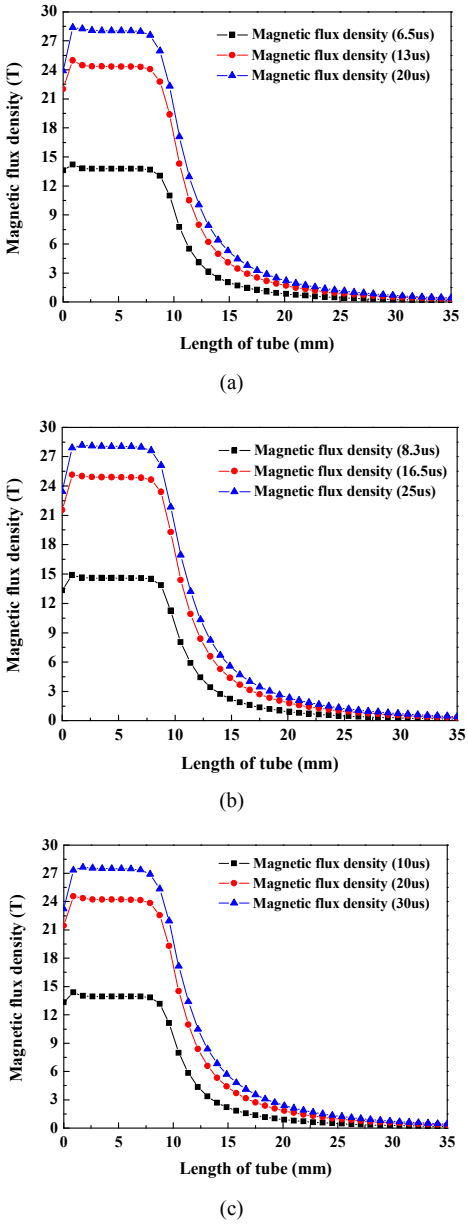

Fig. 10. Magnetic flux density with variation of discharge time: (a) Case A (Discharge time = 20 μs); (b) case B (Discharge time = 25 μs); (c) case C (Discharge time = 30 μs).

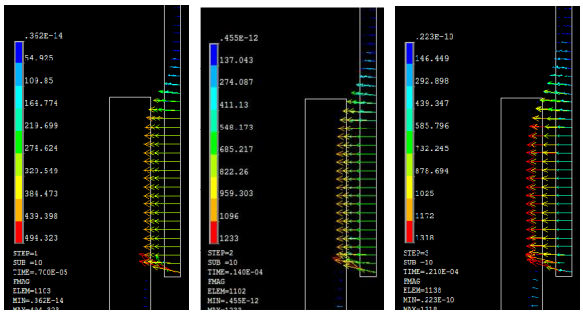

(a) (b) (c)

Fig. 11. Vector plot of the magnetic force at 20 μs discharge time: (a) 6.5; (b) 13 μs; (c) 20 μs.

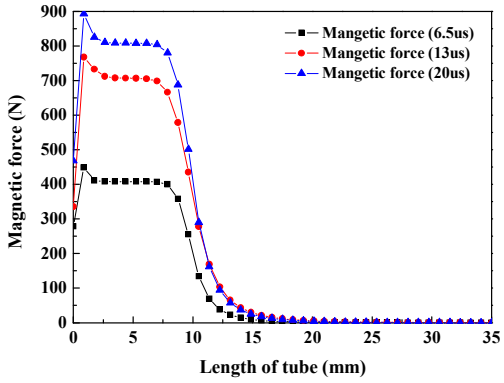

(a)

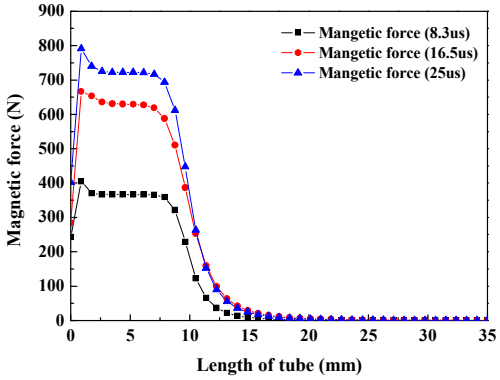

(b)

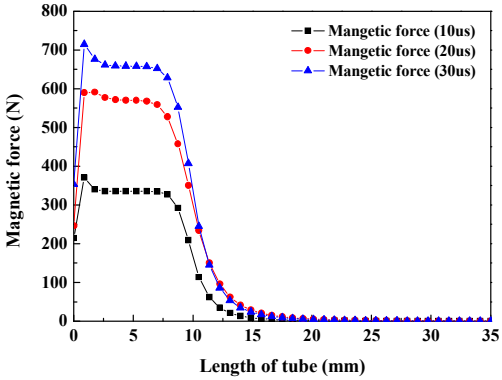

(c)

Fig. 12. Magnetic force with variation of discharge time: (a) Case A (Discharge time = 20 μs); (b) case B (Discharge time = 25 μs); (c) case C (Discharge time = 30 μs).

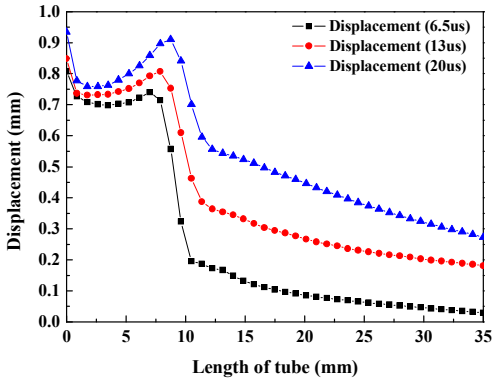

(a)

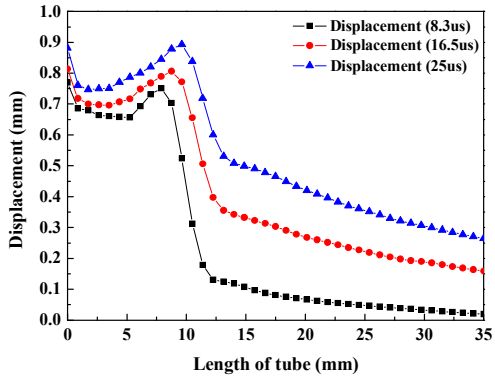

(b)

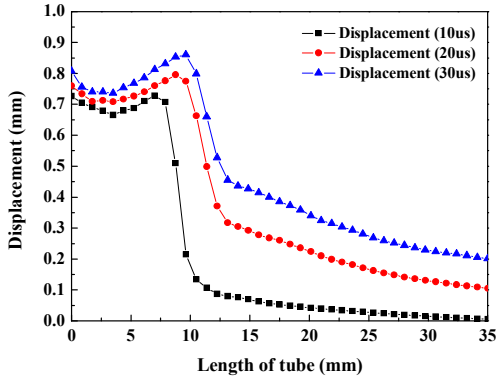

(c)

Fig. 13. Displacement of Al tube with variation of discharge time: Magnetic force with variation of discharge time: (a) Case A (Discharge time = 20 μs); (b) case B (Discharge time = 25 μs); (c) case C (Discharge time = 30 μs).

other words, the electromagnetic force with varied discharge time changed into the energy for plastic deformation and kinetic energy for welding.

Fig. 13 shows the displacement of the Al tube with the variation of discharge time obtained from the simulation. The maximum displacement of the Al tube was observed at the welding start point and was calculated to be 0.93 mm at the 20 μs discharge time. Additionally, the maximum displacements were calculated to be 0.79 mm and 0.84 mm at the 6.5 μs and 13 μs discharge times, respectively. However, the maximum displacements were measured to be 0.88 mm and 0.81 mm at the 25 μs and 30 μs discharge times, respectively. The maximum displacement gap between 20 μs and 30 μs was 0.12 mm. Since the electromagnetic force increases with decreasing discharge time, the displacement of the Al tube also increased sharply. The strain of the Al tube is plotted in Fig. 14. The highest strain was observed at the 20 μs discharge time with the highest electromagnetic force. The maximum strain was calculated to be 0.036 at the 20 μs discharge time,

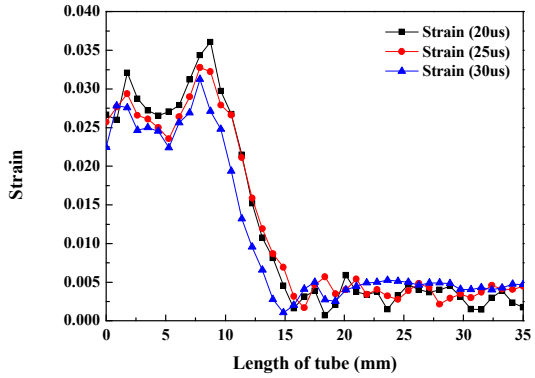

Fig. 14. Strain of Al tube with variation of discharge time.

and the location of maximum strain was 10 mm from the end of the overlap area. Another high strain was measured at 0.325 on 2.5 mm, which was located on the end of the overlap area, but the strain on the center was calculated as 0.026. In contrast, when the discharge times were 25 μs and 30 μs, the maximum strains were 0.032 and 0.031, respectively. These numerical results confirmed that the generated electromagnetic force during the process changed according to the variation of the discharge time, which led to different wavy forms being made on the joint interface in previous experimental works.

4. Conclusions

The effect of discharge time was analyzed using experimental and numerical works, and the following conclusions were reached:

(1) In a tubular joint with MPW, two weld zones were measured in an overlap zone. In particular, the wavy forms that are characteristic of solid-state welding were observed on the Al/Steel interface of the joint, which had various lengths and amplitudes according to the variation of discharge time.

(2) As the capacitance decreased under same charge energy, the discharge time also decreased. Decreasing the discharge time caused the induced current on outer workpiece to increase. Therefore, the electromagnetic force, which means the repulsive force between the inputted current and induced current, can be increased.

(3) Increasing the electromagnetic force led to increasing the deformation of the workpiece, so the length of wavy forms was longer and the amplitude was higher for wavy forms on the interface of the workpiece.

(4) Although a dramatic increment in terms of electromagnetic interaction was not observed, the wave form length and amplitude were clearly distinguished between joints by the discharge times.

Acknowledgment

This work was supported by Ministry of Trade, Industry & Energy (10062301), Korea.

References

[1] J. Y. Shim, I. S. Kim, M. J. Kang, I. J. Kim, K. J. Lee and B. Y. Kang, Joining of aluminum to steel pipe by magnetic pulse welding, *Materials Transactions*, 52 (5) (2011) 999-1002.

[2] Y. B. Park, Design of joints for the automotive spaceframe with electromagnetic forming and adhesive bonding, *The Degree of Doctor of Philosophy,* Graduate School of the Seoul National University (2004) 24-78.

[3] A. Kochan, Magnetic pulse welding shows potential for automotive applications, *Assembly Automation,* 20 (2) (2000) 129-132.

[4] R. M. Miranda, B. Tomás, T. G. Santos and N. Fernandes, Magnetic pulse welding on the cutting edge of industrial applications, *Soldag. Insp. São Paulo*, 19 (1) (2014) 69-81.

[5] H. Hokari, T. Sato, K. Kawauchi and A. Muto, Magnetic impulse welding of aluminum tube and copper tube with various core materials, *Welding International*, 12 (8) (1998) 619-626.

[6] D. Dudko, V. Chudakov, L. Kistersky and T. Barber, Magnetic pulse welding of tubing: Exploring the cold welding process, *The Fabricator*, 26 (8) (1996) 62-65.

[7] Y. Zhang, S. S. Babu, C. Prothe, M. Blakely, J. Kwasegroch, M. LaHa and G. S. Daehn, Application of high velocity impact welding at varied different length scales, *Journal of Materials Processing Technology*, 211 (2011) 944-952.

[8] A. Kapil and A. Sharma, Coupled electromagnetic-structural simulation of magnetic pulse welding, *Proceeding of AIMTDR 2014,* India (2014) 249.1-249.6.

[9] R. N. Raoelison, N. Buiron, M. Rachik, D. Haye and G. Franz, Efficient welding conditions in magnetic pulse welding process, *Journal of Manufacturing Processes*, 14 (3) (2012) 372-377.

[10] J. Bellmann, J. Lueg-Althoff, G. Goevel, S. Gies, E. Beyer and A. E. Tekkaya, Effect of surface coating on the joint formation during magnetic pulse welding in tube to cylinder configuration, *Proceeding of ICHSF2014*, Korea (2014) 275-287.

[11] J. Cui, G. Sun, J. Xu, Z. Xu and X. Huang, A study on the critical wall thickness of the inner tube for magnetic pulse welding of tubular Al-Fe parts, *Journal of Materials Processing Technology*, 227 (2016) 138-146.

[12] J. Lueg-Althoff, B. Schiling, J. Bellmann, S. Gies, S. Schulze, A. E. Tekkaya and E. Beyer, Influence of the wall thicknesses on the joint quality during magnetic pulse welding in tube-to -tube configuration, *Proceeding of ICHSF2016*, Germany (2016) 259-268.

[13] A. Ben-Artzy, A. Stern, N. Frage and V. Shribman, Interface phenomena in aluminum magnesium magnetic pulse welding, *Journal of Science and Technology of Welding and Joining*, 13 (4) (2008) 402-408.

[14] A. Ben-Artzy, A. Stern, N. Frage, V. Shribman and O. Sadot, Wave formation mechanism in MPW, *International Journal of Impact Engineering,* 37 (4) (2010) 397-404.

[15] S. D. Kore, P. P. Date and S.V. Kulkarni, Effect of process parameters on electromagnetic impact welding of aluminum sheets, *Journal of Impact Engineering*, 34 (2007) 1327-1341.
[16] H. Geng, J. Cui, G. Sun and G. Li, A study on the critical thickness of the inner tube for MPW, *Proceeding of ICHSF2014*, Korea (2014) 321-330.
[17] V. Shribman and M. Blakely, Benefits of the magnetic pulse process for welding dissimilar metals, *Welding Journal*, 87 (9) (2008) 56-59.
[18] P. Zhang, Joining enabled by high velocity deformation, *The Degree Doctor of Philosophy,* Graduate School of the Ohio State University (2003) 183-200.
[19] H. G. Powers, Bonding of aluminum by the capacitor discharge magnetic forming processes, *Welding Journal*, 46 (1967) 507-510.
[20] J. Y. Shim, I. S. Kim, K. J. Lee and B. Y. Kang, Experimental and numerical analysis on aluminum/steel pipe using magnetic pulse welding, *Met. Mater. Int*., 17 (6) (2011) 957-961.
[21] ANSYS, *ANSYS reference manual-Release5.7*, ANSYS, USA (1999).
[22] J. O. Hallquist, *LS-DYNA Theoretical Manual*, Livermore Software Technology Corporation, Livermore, USA (1991).

Ji-Yeon Shim earned her master's degree from the Mokpo National University, Korea. Her research interests are magnetic pulse welding simulation and optimization.

Bong-Yong Kang earned his doctor's degree from Inha University, Korea. His research focuses on the magnetic pulse welding and forming process of lightweight materials component.

Ill-Soo Kim earned his doctor's degree from University of Wollongong, Australia. His research focuses on the magnetic pulse welding process of lightweight materials component.